ARTICLES

A Study of the Thermal Decomposition of 2-Azidoacetamide by Ultraviolet Photoelectron Spectroscopy and Matrix-Isolation Infrared Spectroscopy: Identification of the Imine Intermediate $H_2NCOCHNH$

J. M. Dyke,* G. Levita, A. Morris, and J. S. Ogden

Department of Chemistry, University of Southampton, Southampton SO17 1BJ, U.K.

A. A. Dias,† M. Algarra,† J. P. Santos,† M. L. Costa,† P. Rodrigues,‡ and M. T. Barros‡

CEFITEC/CFA, Department of Physics, Faculdade de Ciencias Tecnologia, Universidade Nova de Lisboa, 2829-215 Caparica, Portugal, and CQFB, Department of Chemistry, Faculdade de Ciencias Tecnologia, Universida Nova de Lisboa, 2829-215 Caparica, Portugal

Received: December 5, 2003; In Final Form: March 30, 2004

The thermal decomposition of 2-azidoacetamide ($N_3CH_2CONH_2$) has been studied by matrix-isolation infrared spectroscopy and real-time ultraviolet photoelectron spectroscopy. N_2, CH_2NH, HNCO, CO, NH_3, and HCN are observed as high-temperature decomposition products, while at lower temperatures, the novel imine intermediate $H_2NCOCH{=}NH$ is observed in the matrix-isolation IR experiments. The identity of this intermediate is confirmed both by *ab initio* molecular orbital calculations of its IR spectrum and by the temperature dependence and distribution of products in the photoelectron spectroscopy (PES) and IR studies. Mechanisms are proposed for the formation and decomposition of the intermediate consistent both with the observed results and with estimated activation energies based on pathway calculations.

Introduction

A study of the thermal decomposition of organic azides is important for a variety of reasons, not least because of their potential roles both as explosives and as systems for high-energy storage. As such, their intrinsic instability makes their properties difficult to measure, and experimental work must be carried out with care, ideally being limited to samples in small quantities. Nevertheless, the study of the mechanisms of organic azide thermal decompositions is of considerable interest both from a fundamental viewpoint and because of the important roles played by such azides in heterocycle synthesis[1−3] and biological and pharmaceutical processes.[4−6] They are also used in the preparation of semiconductor materials[7,8] and as high-energy density materials used in solid propellants[9,10] and explosives.[11]

Bock and Dammel[12−16] were among the first workers to study the thermal decompositions of alkyl azides in the gas-phase using UV photoelectron spectroscopy (PES). The main conclusion from this work was that alkyl azide thermal decomposition follows a path in which N_2 evolution is accompanied by a 1,2 shift to form an imine, which can undergo further elimination to produce a nitrile. This process might also be envisaged to proceed stepwise via the formation of the nitrene, but there is no experimental evidence for this. Although the UV photoelectron spectrum of CH_3N, made from decomposition of CH_3N_3, has recently been reported by Dianxun and co-workers,[17] this species was produced by the decomposition of the parent azide on a heated molecular sieve surface in the presence of NO. It appears that there have been no observations of nitrene intermediates from gas-phase azide decompositions. The pyrolysis of CH_3N_3 is therefore envisaged as

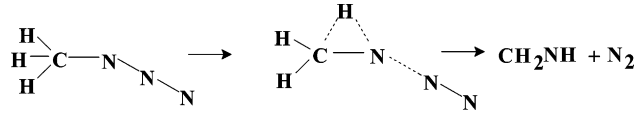

followed by

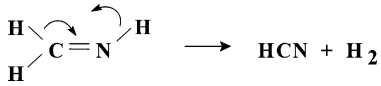

This basic reaction sequence involving an initial 1,2 shift satisfactorily accounts for the range of products found in azides of type $RR'R''CN_3$, where R, R′, and R″ may be H, Me, or allyl,[12,18] and can be described by a "type 1" decomposition pathway. In this process, the migrating group need not necessarily be only H. Thus Me_3CN_3 decomposes to form $Me_2C{=}NMe$, and ultimately MeCN and (probably) C_2H_6.[15,19]

* To whom correspondence should be addressed.
† CEFITEC/CFA, Department of Physics.
‡ CQFB, Department of Chemistry.

10.1021/jp031288s CCC: $27.50
Published on Web 05/22/2004

More recently, further studies on the thermal decomposition of organic azides have been reported using the combined application of PES and matrix-isolation infrared spectroscopy, together with *ab initio* molecular orbital methods,[20−22] and these studies have revealed a second "type 2" mode of azide decomposition. The first system for which this was found to apply was the thermal decomposition of 2-azidoacetic acid,[20] which decomposed to give CO_2 and CH_2NH as important products not expected by the "type 1" mechanism.

For this system, an alternative "type 2" route was proposed as

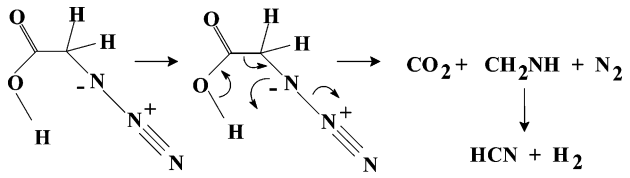

This second decomposition route was subsequently found to be applicable for ethyl azidoacetate decomposition [22] and also for some of the products identified in the pyrolysis of azidoacetone.[21]

This paper describes related studies on the pyrolysis of 2-azidoacetamide using the techniques of real-time ultraviolet photoelectron spectroscopy and matrix-isolation infrared spectroscopy, supported by *ab initio* molecular orbital calculations. The main aim is to investigate the mechanism of thermal decomposition by obtaining spectra at different temperatures and so perhaps detect not only the final products of pyrolysis but also any intermediates; this may lead to a greater understanding of the decomposition process.

Experimental Section

Preparation and Characterization of $N_3CH_2CONH_2$. Samples of 2-azidoacetamide were obtained from the reaction of chloracetamide with sodium azide under aqueous conditions. In a typical reaction, ca. 2.0 g of chloroacetamide was added slowly to a solution of sodium azide (3 equiv) in water. The mixture was stirred for 24 h in an oil bath at 60 °C. After cooling, the product was extracted with ethyl acetate, and the organic phase was dried over anhydrous sodium sulfate and concentrated using a rotary evaporator.

2-Azidoacetamide ($N_3CH_2CONH_2$) is a white crystalline solid at room temperature. It was purified by recrystallization from dichloromethane (mp 55−56 °C) and was characterized in the vapor phase by ultraviolet photoelectron spectroscopy (PES) and electron-impact mass spectrometry, in solution by ^1H and ^{13}C NMR (Bruker AMX-400), and in the solid phase by IR spectroscopy (Nujol mull−Mattson Satellite FT-IR).

The 70 eV electron-impact mass spectrum displayed a parent peak at 100 amu (2.1%) and stronger peaks at 28 (N_2^+, CH_2N^+, 100%), 44 ($CONH_2^+$, 17.1%) and 72 ($NCH_2CONH_2^+$, 2.6%) amu. Signals were present also at 29 (HCO^+, 4.9%) and 43 ($HNCO^+$, 2.6%) amu. In the 20 eV electron-impact mass spectrum, the relative intensities of all the ions were enhanced with respect to the N_2^+ intensity. The relative intensity for the parent ion was 14.8%, for $CONH_2^+$ 100%, for $NCH_2CONH_2^+$ 24.8%, for HCO^+ 20.9%, and for $HNCO^+$ 4.8%.

The ^1H NMR spectrum ($CDCl_3$ solution) shows a singlet at 4.01 ppm relative to TMS corresponding to the methylene group and a broad (1:1) doublet at 6.46 ppm assigned to the NH protons. The ratio between the CH_2 and NH_2 signal intensities was 1.04:1. The doublet observed for the NH_2 signal is attributed to the two $-NH_2$ protons being chemically inequivalent. The ^{13}C NMR spectrum ($CDCl_3$ solution) shows peaks at 52.7 ppm (relative to TMS) assigned to the methylene carbon and at 170.2 ppm, which is assignable to the carbonyl carbon.

The most significant features in the Nujol mull IR spectrum (KBr plates) were a broad doublet at 3373 and 3179 cm^{-1} assigned to N−H stretching modes, C−H stretching modes at 2980−2920 cm^{-1} (overlapping with Nujol bands), and prominent bands at 2117 cm^{-1} (N_3 stretching), 1630 cm^{-1} (C═O stretching), and 1414 cm^{-1}.

Matrix-Isolation IR Studies. Matrix-isolation infrared studies followed a very similar pattern to those described for previous studies on organic azides.[20−22] The inlet and pyrolysis parts of the apparatus were identical, as were the low-temperature Displex and IR spectrometers. However, although spectra could generally be obtained with the parent azide maintained at room temperature, it was often convenient to warm the sample and inlet system to ca. 300 K to generate a more satisfactory flux of material. Spectra of the parent azide and its decomposition products were obtained in nitrogen matrices, and supporting experiments were also carried out on NH_3/N_2 and H_2NCHO/N_2 to augment our N_2 matrix infrared data bank of known molecular vibration frequencies. Deposition times were typically 30−60 min at a particular superheater temperature, and any changes occurring during this period were monitored by spectral subtraction.

Matrix ratios were estimated to be well in excess of 1000:1.

Photoelectron Spectroscopy. The photoelectron spectra obtained for 2-azidoacetamide were recorded using the single-detector instrument described elsewhere,[23] specifically built for high-temperature decomposition studies. All the spectra were recorded using He Iα radiation (21.22 eV). In contrast to previous PES studies on the organic azides 2-azidoacetone, 2-azidoethanol, and 2-azidoethyl acetate,[21,22] 2-azidoacetamide has insufficient vapor pressure at room temperature to allow photoelectron spectra to be recorded with acceptable signal-to-noise by simply pumping on the sample held in a flask outside the ionization chamber of the spectrometer. As in the case of 2-azidoacetic acid,[20] it was necessary to preheat the sample inside the ionization chamber to achieve a sample vapor pressure in the photoionization region, which was high enough to give spectra with acceptable signal-to-noise ratios. This was achieved by placing solid azidoacetamide samples in a small, noninductively wound, resistively heated furnace placed above both the radio frequency (rf) pyrolysis tantalum furnace and the photon beam in the ionization chamber of the spectrometer. Photoelectron spectra of the parent azide were calibrated using argon and methyl iodide[24] added to the ionization chamber at the same time as the azide vapor samples. The photoelectron spectrum of the azide precursor, chloroacetamide, was also recorded and calibrated using methyl iodide and argon. This was done to test for the possible presence of this impurity in the azide spectra. In practice, all parent azide spectra were free from any detectable trace of the precursor used in the preparation. The wall temperatures of the resistively heated and the lower rf furnace were measured in each case by a K-type thermocouple placed in contact with the walls. The pressure of the azide in the ionization region was estimated as ca. 10^{-4} Torr under conditions at which pyrolysis experiments were started, and the flight time between the pyrolysis region and the photoionization region was estimated as ca. 5 ms, and from the length of the pyrolysis zone, the residence time in this region is estimated as 3 ms.

The thermal decomposition of 2-azidoacetamide was monitored by PES in real time by slowly increasing the temperature of the rf pyrolysis region with a fixed temperature of the

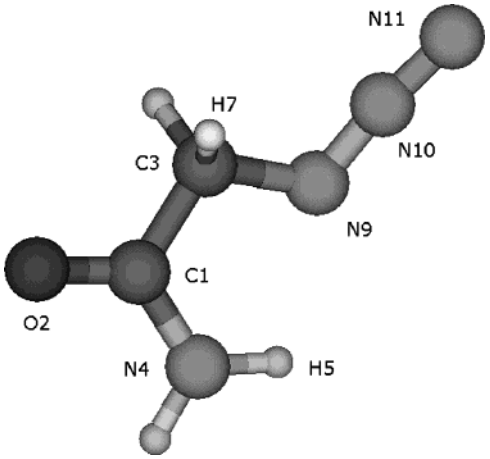

Figure 1. Structure of cis−cis conformer of 2-azidoacetamide.

resistively heated furnace, the onset of pyrolysis being marked by the appearance of characteristic N_2 bands, an associated lowering of the parent azide bands, and an increase in other features associated with the pyrolysis products. At this stage, a further spectral calibration was made using the vertical ionization energies (VIEs) of the first bands of N_2, H_2O, or HCN.[24]

Molecular Orbital Calculations. To assist interpretation of the photoelectron and infrared spectra, molecular orbital calculations were carried out on the parent azide and on the imine $H_2NCOCH{=}NH$ with the aim of establishing equilibrium geometries and then to calculate vertical ionization energies (VIEs) and infrared frequencies and intensities. These calculations were carried out at the MP2/6-31G** level. For the VIEs, Koopmans' theorem was applied to the SCF orbital energies obtained at the MP2/6-31G** geometry, and the values obtained were scaled by a factor of 0.92.[25,26] Also, some of the lower VIEs were calculated with the ΔSCF method. Harmonic vibrational frequencies were calculated at the MP2/6-31G** level via second-derivative calculations. These frequencies are expected to be high (by ca. 5%) because only partial allowance has been made for electron correlation in the method used.[27−29] Also, no corrections were made for anharmonicity in comparing the computed harmonic frequencies with the experimental frequencies.

Results and Discussion

Calculated Equilibrium Geometry of 2-Azidoacetamide. At the MP2/6-31G** level of calculation, four minimum energy conformers were found for $N_3CH_2CONH_2$ in its closed-shell singlet state, the relatively small energy differences arising from the different relative orientations of the carbonyl, methylene, and azide groups. The most stable predicted geometry is shown in Figure 1 and is described as the cis−cis conformer. The most important structural parameters of this conformer and the relative energies of the four minimum energy conformers are summarized in Table 1.

Observed and Calculated VIEs of 2-Azidoacetamide. Figure 2 shows a typical photoelectron spectrum of 2-azidocetamide. Eight distinct bands may be readily identified and are labeled A−H in this figure. VIEs were determined by averaging the VIEs measured from nine different spectra.

Table 2 reports the first nine VIEs for the most stable conformer (structure cis−cis), calculated using Koopmans' theorem and scaled by a factor of 0.92 and two VIEs calculated with the ΔSCF method by optimizing the geometry of the cation. These calculations are in satisfactory agreement with the experimental spectrum and indicate that bands B and F both arise from overlap of two one-electron ionizations.

Of the four minimum energy structures located at the MP2/6-31G** level, three of these structures differ by less than 2.0 kcal mol^{-1}, while the trans−cis structure lies approximately 5.2 kcal mol^{-1} higher than the most stable (cis−cis) structure. The

TABLE 1: Geometrical Parameters for the Lowest Energy Structure of 2-Azidoacetamide[a] and Total Energies of the Four Minimum-Energy Structures of Azidoacetamide at the MP2/6-31G Level**

Geometrical Parameters for the Lowest Energy Structure

bond	length (Å)	angle	value (deg)
N11−N10	1.163	N11−N10−N9	173.2
N10−N9	1.2455	N10−N9−C3	115.52
N9−C3	1.4776	N9−C3−H7	111.25
C3−H7	1.0913	N9−C3−C1	110.65
C3−C1	1.5243	O2−C1−N4	124.87
C1−O2	1.2291	C1−N4−H5	119.1
C1−N4	1.3573	N10−N9−C3−C1	189.3
N4−H5	1.0059	N9−C3−C1−O2	191.6

Total Energies of the Four Minimum-Energy Structures

structure	energy (au)	rel. energy (kcal mol^{-1})
trans−trans	−371.761 257	1.96
cis−cis	−371.764 376	0.0
cis−trans	−371.764 112	0.16
trans−cis	−371.756 125	5.18

[a] See Figure 1 for the numbering of the atoms.

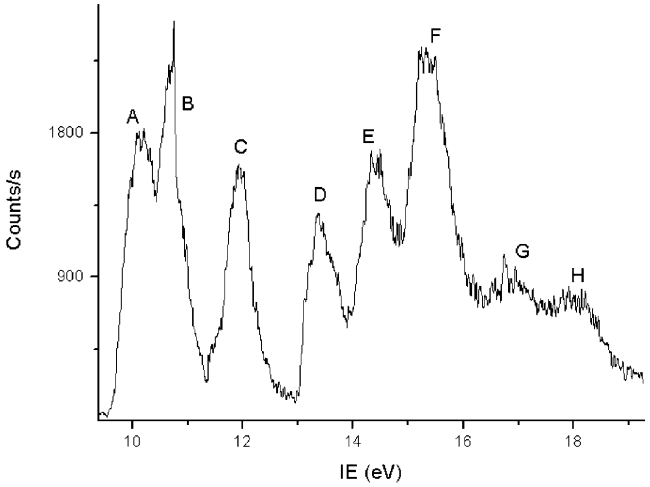

Figure 2. He I PE spectrum of 2-azidoacetamide at sample temperature of 320 K.

TABLE 2: Experimental and Computed VIEs of the Lowest Energy Structure of 2-Azidoacetamide

KT calcd VIE (eV)[a]	KT calcd 0.92 × VIE (eV)	ΔSCF calcd VIE (eV)	exptl VIE (eV)	band[b]
10.69	9.83	10.24	10.16	A
11.34	10.43		10.68	B
11.70	10.76	10.40		
12.57	11.56		11.94	C
14.75	13.57		13.37	D
15.97	14.69		14.44	E
17.11	15.75		15.35	F
17.52	16.11			
18.38	16.91		16.93	G
19.09	17.56		17.99	H

[a] Koopmans' theorem (KT) values (see refs 25 and 26). [b] See Figure 2 for the lettering of the bands.

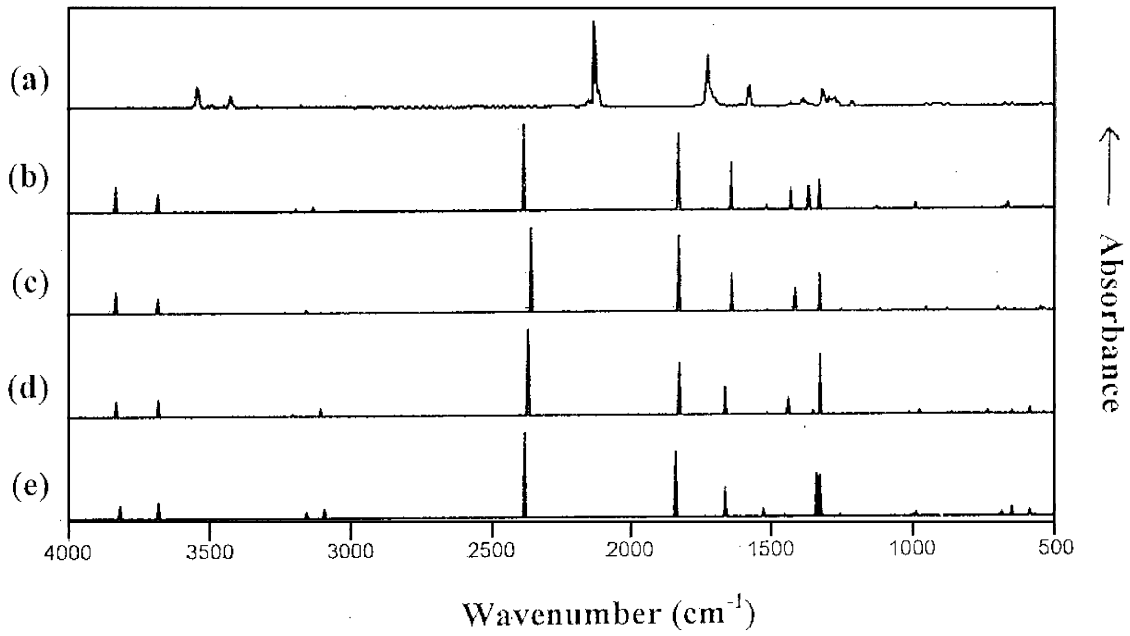

Figure 3. Nitrogen-matrix IR spectrum (a) of 2-azidoacetamide and calculated IR spectra of (b) cis−cis conformer, (c) cis−trans conformer, (d) trans−cis conformer, and (e) trans−trans conformer of 2-azidoacetamide.

description used here reflects the relative positions (cis or trans) of the methylene hydrogens relative to the oxygen atom and of the azide chain relative to the methylene hydrogens (cis or trans). For example, Figure 1 shows the cis−cis structure with the $-CH_2$ group and the $-N_3$ group cis to each other and the $-CH_2$ and C═O groups cis to each other. Because of the small differences in energy between the conformers cis−cis, trans−trans, and cis−trans, it is possible that these three structures all contribute to the experimental gas-phase spectrum. Valence vertical ionization energies have been computed for these structures using Koopmans' theorem, and they were found to be very similar.

Observed and Calculated IR Spectra of 2-Azidoacetamide. Figure 3a shows a typical nitrogen-matrix infrared (IR) spectrum obtained for 2-azidoacetamide. Prominent bands are found at 3538, 3420, 2126, 1719, and 1574 cm^{-1}, bands that are at similar, though somewhat higher, positions to those recorded for the Nujol mull spectrum of the solid. The most significant difference is the considerably higher frequency of the two N−H stretching modes (3538 and 3420 cm^{-1} in the matrix compared with 3373 and 3179 cm^{-1} in the solid), and this almost certainly arises from the lack of intermolecular hydrogen bonding in the matrix-isolated species.

Figure 3b shows the calculated IR spectrum for the lowest energy cis−cis conformer, and apart from the anticipated errors in absolute band position, the overall agreement with respect to band intensities and general appearance is satisfactory and lends credence to the use of our calculations in supporting the identification of molecular species of this type.

Calculations were also carried out on the three other low-energy conformers found for 2-azidoacetamide, but these did not reproduce the experimental spectrum quite as well. The computed spectra for these conformers are also shown in Figure 3. Comparison with the experimental spectrum (Figure 3a) is least satisfactory for the trans−cis structure (the highest energy structure) and the trans−trans structure (the next highest energy structure), notably in the N−H stretching region (3300−3900 cm^{-1}) and the 2400−1200 cm^{-1} region. The computed values are all slightly higher than the experimental values because of only partial allowance for electron correlation in the calculations and neglect of anharmonicity; this latter effect is expected to be particularly important for N−H and C−H stretches.

Thermal Decomposition Experiments: IR Spectroscopy. Figure 4 shows typical nitrogen-matrix infrared spectra obtained from a sample of $N_3CH_2CONH_2$ for a series of increasing pyrolysis temperatures. At the lowest temperature (300 K), the only absorptions detected are those of the parent (the most prominent bands are denoted P), together with the two most intense IR features of matrix-isolated water−denoted by an asterisk (∗). Such traces of water are typically observed from organic azide samples, and they most probably arise either as a result of residual water in the parent azide or as a result of desorption from the inner glass surfaces of the heated inlet system.

Pyrolysis experiments were carried out in the range ca. 400−800 K, and at the relatively low temperature of 470 K, there is evidence for the presence of a pyrolysis product characterized by a weak band at 869 cm^{-1}. Further heating in the range 540−590 K shows a significant reduction in the prominent azide peak at 2126 cm^{-1} and the growth of at least 10 significant features.

One of these, labeled A, is identified as HNCO by comparison with previous studies,[30] but the remaining new bands, labeled I, have not previously been seen in our IR pyrolysis studies. They are tentatively assigned to a common species on the basis of their reproducible relative intensity ratios over a range of experimental conditions.

Yet further heating (650−800 K) results in a decrease of bands I, and the continued growth of well-established features due to HCN (bands B), CO (band C), CH_2NH (bands D), and NH_3 (band E), together with a second band of HNCO (also labeled A). Table 3 summarizes the positions and assignments of the bands observed in these experiments.

These pyrolysis runs were very reproducible and indicate that although the final decomposition products are well-established, they are formed via an intermediate (bands I) that has some structural features in common with the parent azide, notably the ketonic CO group and the NH_2 unit. This intermediate is present over a relatively well-defined temperature range (ca. 500−700 K), and its decomposition appears to result in the formation of *all* the remaining species identified.

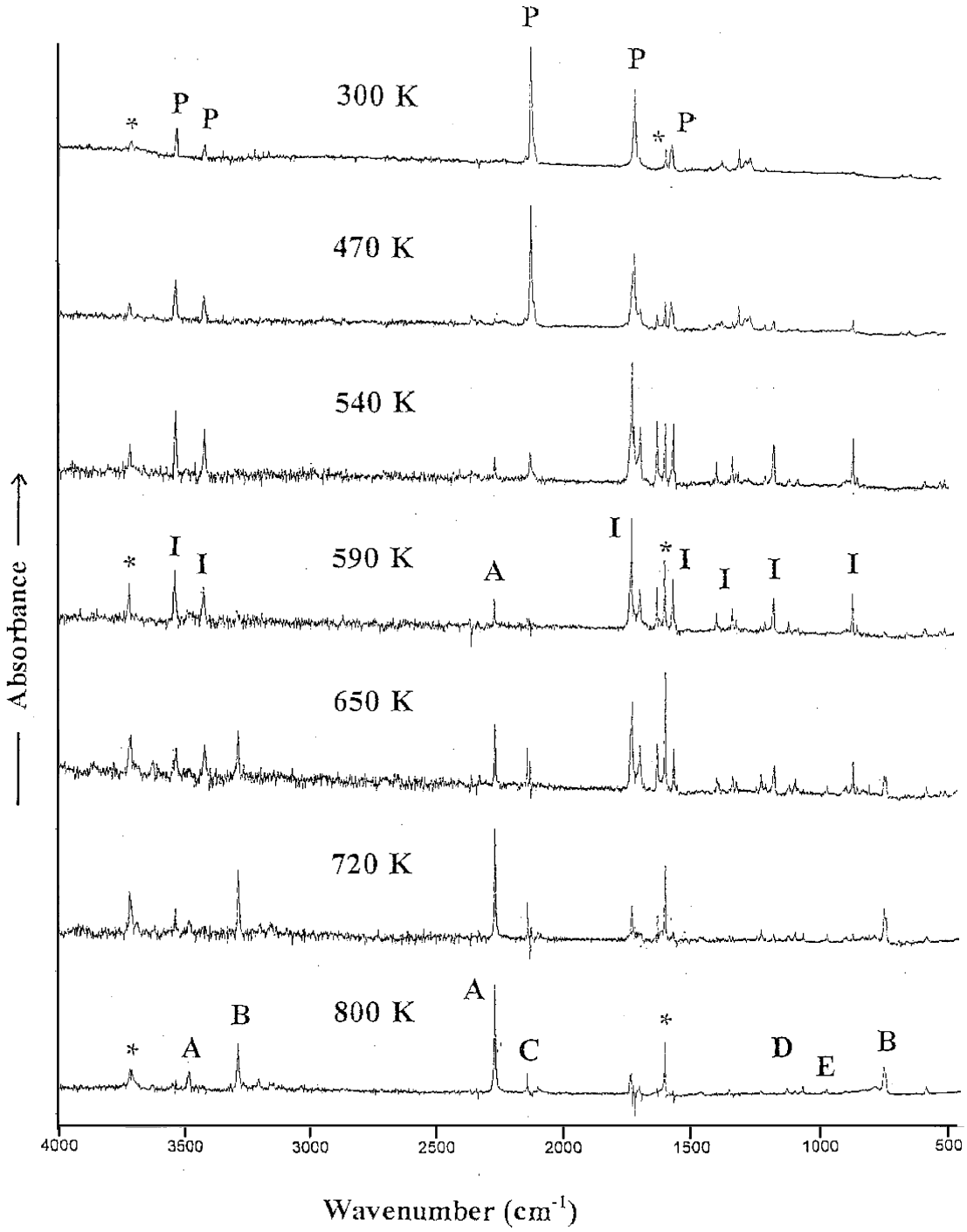

Figure 4. Sequence of nitrogen matrix IR spectra obtained from pyrolysis of 2-azidoacetamide over the temperature range 300−800 K (band identification given in Table 3).

Thermal Decomposition Experiments: Photoelectron Spectroscopy. Figure 5a,b shows typical photoelectron spectra obtained at increasing temperatures, reflecting an increasing degree of pyrolysis of 2-azidoacetamide from 0% at 320 K to ca. 100% at 870 K.

The first evidence of pyrolysis was the appearance of the first band of molecular nitrogen at 15.58 eV (VIE),[24] and by 550 K, Figure 5a, the N_2 bands are relatively intense, and features arising from three additional pyrolysis products appear simultaneously. The broad band at 10.66 eV (VIE) and a vibrationally resolved band at 12.50 eV (VIE) are both attributed to CH_2NH.[16,31] The vibrationally resolved band at 11.61 eV (VIE equal to AIE) is attributed to HNCO,[32] and a weak feature due to HCN is also present. At 870 K, Figure 5b, the parent azide bands have essentially disappeared. Further heating, ultimately to ca. 1100 K, resulted in the eventual disappearance of all the above bands, apart from HCN and N_2, and the growth of a band due to CO.

It is notable that HCN and CH_2NH are both observed *early* in the pyrolysis at approximately the same (modest) furnace temperature, and it is evident that, unlike the azidoacetic acid system,[20] HCN is not produced here from CH_2NH.

No features were observed in these PES studies that could be attributed to either an imine intermediate, $H_2NCOCHNH$, or a possible nitrene precursor, H_2NCOCH_2N (in either a singlet or a triplet state). However, from ΔSCF calculations at the

TABLE 3: Significant IR Bands (cm^{-1}) Observed in Matrix Isolation Studies on the Pyrolysis of 2-Azidoacetamide

N_2 matrix (Figure 3)[a]	previous studies	assignment
P: 3538, 3420, 2126, 1719, 1574		$N_3CH_2CONH_2$
I: 3538, 3418, 1728, 1566, 1399, 1339, 1178, 869		$H_2NCOCHNH$
C: 2139	2139	CO[34]
A: 3483, 2265	3483, 2254[b]	HNCO
D: 3032, 2919, 1637, 1450, 1352, 1127, 1065	3033, 2920, 1637, 1450, 1353, 1128, 1065	CH_2NH[35]
B: 3287, 747/737	3287, 747/737	HCN[36]
E: 970	970 (most intense)	NH_3[37]

[a] Wavenumber accuracy ± 1 cm^{-1}. [b] Xe matrix data.[30]

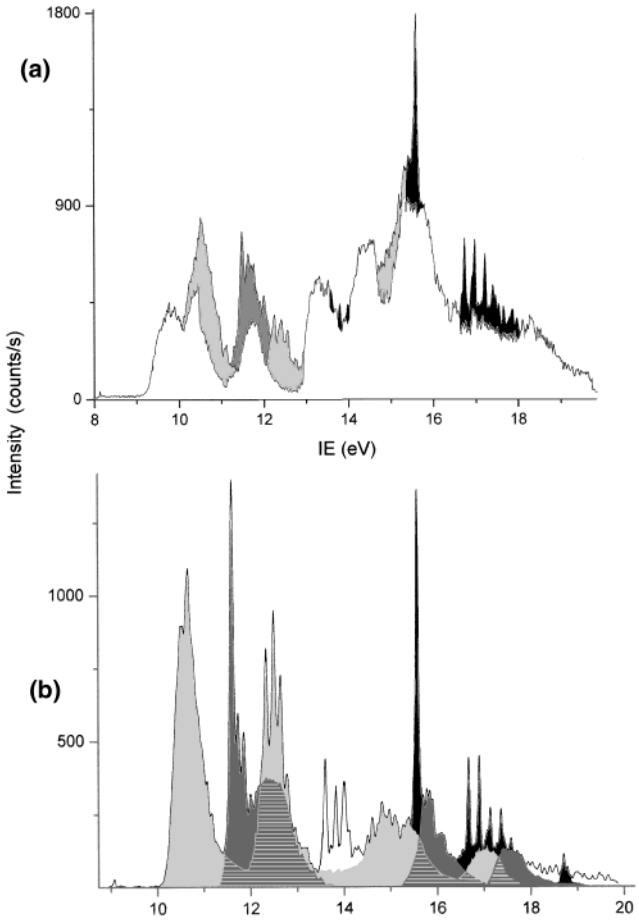

Figure 5. PE spectra obtained from pyrolysis of 2-azidoacetamide: (a) at 550 K, estimated contributions of species are (white shadow) 2-azidoacetamide, (light gray shadow) CH_2NH, (dark gray shadow) HNCO, and (black shadow) N_2 and HCN; (b) at 860 K, estimated contributions of species are (light gray shadow) CH_2NH, (dark gray shadow) HNCO, (white shadow) HCN, and (black shadow) N_2.

6-31G** level, the photoelectron bands for these species are expected to be very close in energy to those of the parent azide, and they could easily be obscured. The computed values for the two first VIEs of these compounds are 9.94 and 10.11 eV for $H_2NCOCHNH$ in its X $^1A'$ state and 9.65 and 10.16 eV for H_2NCOCH_2N in its X $^3A''$ state. Another potential pyrolysis product, formamide, (see later) was also not observed in these experiments. If formamide had been present to any significant extent, then a vibrationally resolved band should have been observed at a position (10.13 eV[24]) quite different from the bands of the parent azide.

Characterization of the Imine Intermediate $H_2NCOCHNH$. As indicated above, the IR spectral sequence shown in Figure 4 indicates the formation and decay of an intermediate, **I**, in the pyrolysis of 2-azidoacetamide. Also, although this intermediate was not detected in the PES experiments, it is significant that intense bands due to molecular N_2 were detected in these experiments at an early stage in the pyrolysis sequence.

The assignment of **I** as the imine $H_2NCOCHNH$, formed via a "type 1" reaction involving the elimination of N_2 and a 1,2 H-atom shift, was initially based on the observed growth and decay patterns shown in Figure 4, and this assignment was subsequently supported by the results of the simulated IR spectrum of this compound.

Figure 6a shows a nitrogen-matrix IR spectrum obtained at a pyrolysis temperature of 590 K, in which all features except bands believed to be associated with **I** have been removed. This spectrum is unlikely to be the *complete* spectrum of **I** but should be representative of the most intense IR features.

Calculations on the various possible conformers of $H_2NCOCH{=}NH$ yielded four distinct structures, each with all real frequencies at the MP2/6-31G** level on a closed-shell singlet surface. The two most stable structures, cis−cis (ground-state configuration) and trans−trans, differ by less than 1.7 $kcal{\cdot}mol^{-1}$, while structures cis−trans and trans−cis lie 5.3 and 7.7 $kcal{\cdot}mol^{-1}$, respectively, above the ground state. In these structures, the description used reflects the relative positions of the C−H hydrogen to the oxygen atom (cis or trans) and of the imine hydrogen to the C−H hydrogen (cis or trans).

Figure 6b shows the IR spectrum calculated for the lowest energy cis−cis conformer of $H_2NCOCHNH$. Although there are discrepancies in band positions, notably in the higher frequency region, the overall agreement between this spectrum and that assigned to species **I** (Figure 6a) is relatively good, and *comparable with that found between the observed and calculated spectra for the parent azide*, (Figure 2). The computed spectra for the other three conformers show poorer agreement with the experimental spectrum, particularly in the N−H stretching region (3800−3400 cm^{-1}) and in the region 1800−1200 cm^{-1}.

Some differences, however, may be noted between the observed and cis−cis calculated spectra. In particular, the observed spectrum (Figure 6a) contains four features in the 1500−2000 cm^{-1} region, while only three are calculated, and additional weak features in the region 500−1500 cm^{-1} are also found in the experimental spectrum. However, all the calculated bands can be matched to features in the experimental spectrum.

We believe that these differences do not negate the identification of **I** as the imine intermediate, but rather that they suggest the possible trapping of more than one conformer in the matrix. Indeed, if the computed spectrum for the second lowest-lying conformer (the trans−trans structure) is taken into account, there is ample flexibility to fit the experimental spectrum at this level of agreement. Support for this view comes from a detailed comparison of the observed and calculated IR spectra for the parent azide (Figure 2), where the observed spectrum between 1300 and 1600 cm^{-1} also shows more features than predicted by calculation and where there is a similar possibility of more than one trapped conformer.

Mechanisms of Gas-Phase Decomposition. The PES experiments show that molecular N_2 is evolved at an early stage in the pyrolysis process, whereas the IR matrix-isolation experiments suggest that the onset of pyrolysis is characterized by the formation of the imine intermediate, $H_2NCOCHNH$, *prior*

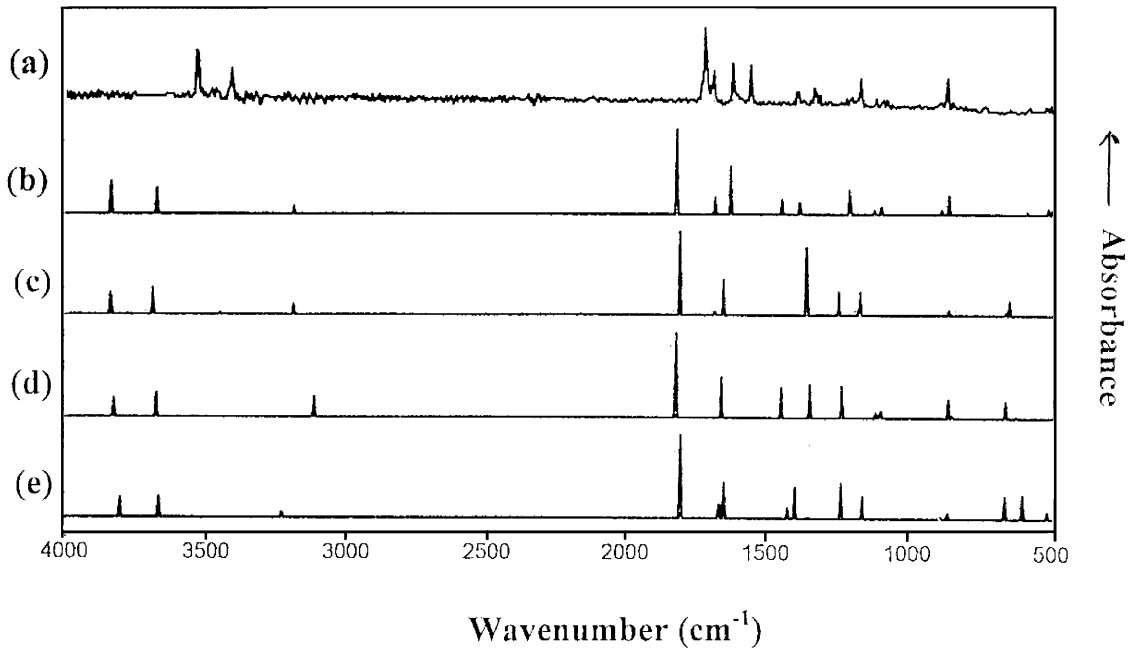

Figure 6. Nitrogen matrix IR spectrum (a) of imine intermediate **I** and calculated IR spectrum for (b) cis−cis conformer, (c) cis−trans conformer, (d) trans−cis conformer, and (e) trans−trans conformer of $H_2NCOCHNH$.

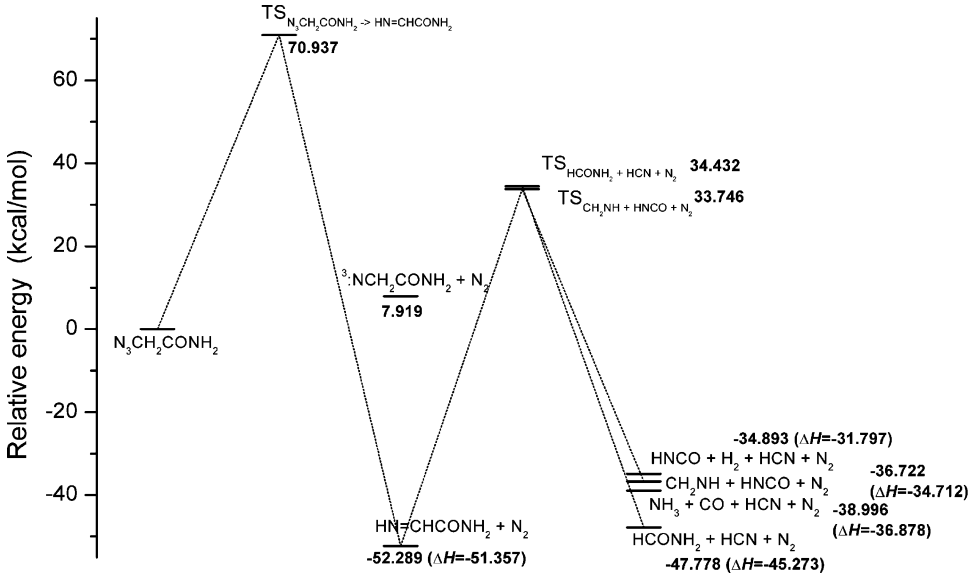

Figure 7. Energy level diagram (at 298 K) showing relative enthalpies of the most stable conformers of 2-azidoacetamide, $H_2NCOCHNH$, and principal decomposition products calculated at the MP2/6-31G** level. The energy of the optimized geometry of the triplet nitrene, obtained from the parent azide on loss of N_2, is also shown in this figure. Geometry optimization calculations of the singlet nitrene all converged to the singlet imine, $HN{=}CHCONH_2$.

to the formation of any other product. Also, what is clear is that, in contrast to some earlier systems,[20−22] CH_2NH cannot be the precursor of the relatively low-temperature formation of HCN.

The initial thermal decomposition process is therefore consistent with the traditional "type 1" route:

$$H_2NCOCH_2N_3 \rightarrow H_2NCOCHNH + N_2$$

Subsequent reaction is then determined by the decomposition of the imine intermediate, and by analogy with the work of Bock and Dammel,[12−16] one might anticipate elimination of HCN and the production of formamide, H_2NCHO.

$$H_2NCOCHNH \rightarrow H_2NCHO + HCN \quad \text{(route A)}$$

However, H_2NCHO was not detected in either the PES or matrix IR studies, and we believe that this is due to the thermal instability of formamide produced under the conditions at which the intermediate **I** begins to decompose.

Matrix IR experiments on the pyrolysis of H_2NCHO performed in this work clearly established that this compound *partially* decomposes into HNCO at ca. 600 K. This observation is consistent with thermochemical data,[38] from which it is possible to show that at this temperature, the Gibbs free energy change is close to zero for the reaction

$$H_2NCHO \rightarrow HNCO + H_2$$

One might therefore expect to observe at least some H_2NCHO during the pyrolysis sequence.

The fact that formamide was *not observed at all* during azide pyrolysis implies a very short lifetime under the conditions used. A similar "premature" decomposition of CH_2NH (into HCN) has previously noted by Bock and Dammel[15] in the pyrolysis of CH_3N_3. If a similar phenomenon is occurring here, the observable products of imine decomposition by this route are therefore expected to be HCN and HNCO. The third product, molecular H_2, is effectively undetectable, as discussed previously.[21]

The overall route

$$H_2NCOCHNH \rightarrow HNCO + HCN + H_2$$

therefore accounts for the presence of two important high-temperature products (HNCO and HCN) but does not account for the formation of CH_2NH, CO, or NH_3.

Two alternative imine decomposition routes can, however, be proposed that might account for these products. These may be termed route B

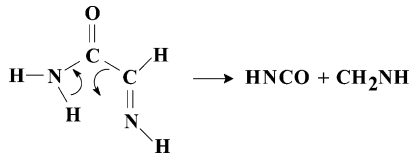

and route C

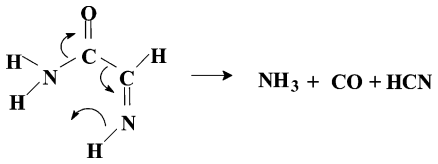

Finally, it is possible to postulate a fourth competing reaction in which azide decomposition follows a "type 2" route, which does not involve imine intermediate **I**:

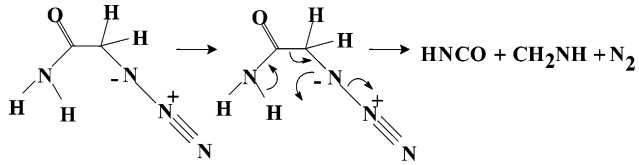

This route, however, does not account for the relatively "early" production of HCN in the pyrolysis sequence (e.g., see Figure 4).

To investigate the various proposed mechanisms of imine decomposition, *ab initio* pathway calculations were carried out at the MP2/6-31G** level, and the results are summarized in Figure 7. Here, the computed relative energies of the reagents, products, and transition states are depicted for the production of the imine from the initial azide and for decomposition routes A and B. Geometry optimization of the singlet nitrene converged to the singlet imine. Also, the enthalpy for conversion of the azide to the triplet nitrene and N_2 was calculated as +8.5 kcal mol^{-1}, higher than that for conversion of the azide to the singlet imine and N_2 (see Figure 7), probably because of stabilization of the imine by delocalization between the C═O and CH═NH bonds.

The transition state linking the azide to the imine is shown in Figure 8a and indicates that the 1,2 H-atom shift occurs before complete N_2 release. For imine decomposition via route A, which ultimately produces HCN, HNCO, and H_2, the transition state is planar (Figure 8b) and is derived most easily from the cis−trans form of the imine, a configuration that is achieved from the predicted cis−cis ground state by rotation. Decomposition is predicted to occur initially to give HNC (which isomerizes to HCN) and H_2NCHO (which decomposes to HNCO + H_2). The production of HNC, HNCO, and H_2 is thus very similar to the production of HNC, CO_2, and H_2 via a proposed concerted mechanism from HNCHCOOH, which is thought to be a minor channel in the decomposition of azidoacetic acid.[33] For route B, decomposition to HNCO + CH_2-NH is predicted to go through a nonplanar transition state, which can be derived directly from the cis−cis form of the imine **I** (Figure 8c).

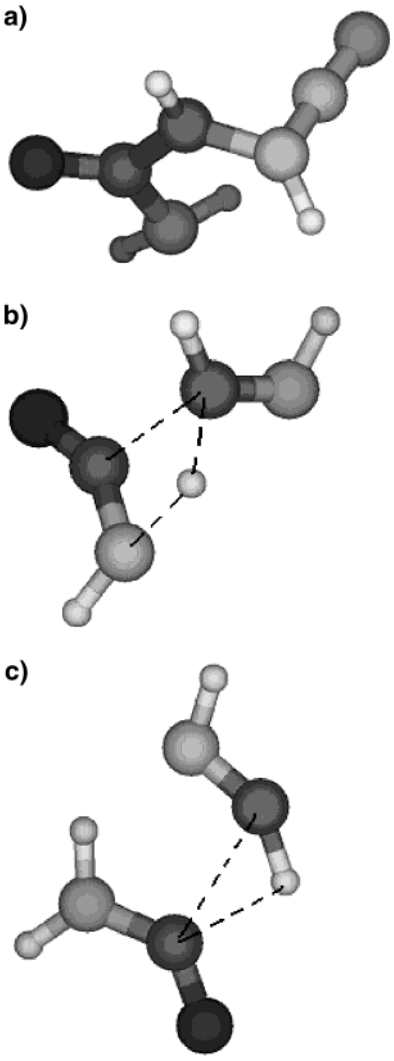

Figure 8. Calculated geometries (at the MP2/6-31G** level) of the transition states for the reactions (a) azide → imine, (b) imine → CH_2-NH + HNCO, and (c) imine → H_2NCHO + HNC.

The activation barriers for both these transition states are predicted to be approximately the same (Figure 7), suggesting that they are both involved simultaneously in imine decomposition, a prediction that is consistent with the experimental observations. Route C is also favorable energetically, but attempts to locate a possible transition state were not successful.

The computed standard relative enthalpies of the products of mechanisms A−C are displayed on the right-hand side of Figure 7 and are in the expected order based on the available thermochemical data.[38] This order places H_2NCHO + HCN + N_2 lower than HNCO + H_2 + HCN + N_2, to the extent of ca. 13 kcal/mol. However, when entropy effects at a pyrolysis temperature of 600 K are taken into account, the Gibbs free

energies are almost identical. At higher temperatures, the HNCO route is lower in free energy.

For the decomposition of the imine to the products, the barriers from the imine to the transition states would be expected to control the product distribution for several competing routes. However, for the two transition states located, these are computed to be very close in energy (see Figure 7). At 600 K, one might therefore expect to see evidence for routes A, B, and C. However as discussed previously, we believe that total decomposition of H_2NCHO may be taking place in this system because of the temperature used and the excess energy arising from the azide decomposition. It is, however, acknowledged that the activation energies, computed at the MP2 level and shown in Figure 7, are likely to be too high because the transition states are almost certainly better represented by a multireference method.

Conclusions

2-Azidoacetamide has been synthesized and characterized by IR spectroscopy, ^1H and ^{13}C NMR, and mass spectrometry, together with IR matrix-isolation and UV photoelectron spectroscopy, and these latter techniques were subsequently used to monitor its thermal decomposition. The experimental results indicate that the dominant route for decomposition of the azide is stepwise, involving first the formation of an imine and molecular nitrogen, followed by at least three imine decomposition pathways. *Ab initio* molecular orbital calculations have been performed, which result in satisfactory agreement between calculated and experimental IR spectra of both of the parent azide and the novel imine intermediate, $H_2NCOCH{=}NH$, formed initially on decomposition. At higher temperatures, this intermediate decomposes to a number of simpler molecules, notably HCN and HNCO, and mechanisms are proposed that account for the sequence of experimental observations.

Acknowledgment. The work reported in this paper was carried out as part of the Reactive Intermediates RTN EC Network. Financial support from the Leverhulme Trust is also acknowledged. The authors are grateful to Dr. E. P. F. Lee for valuable discussions. Also, support from the POCTI grant (Grant 1999/FIS/35526) is gratefully acknowledged.

References and Notes

(1) Patai, S. *The Chemistry of the Azide Group*; Interscience: New York, 1971.
(2) Scriven, E. F. V.; Turnbull, K. *Chem. Rev.* **1988**, *88*, 298.
(3) Vantinh, V.; Stadlbauer, W. *J. Heterocycl. Chem.* **1966**, *33*, 1025.
(4) Maurus, R.; Bogumil, R.; Nguyen, N. T.; Mauk, A. G.; Brayer, G. *Biochem. J.* **1988**, *332*, 67.
(5) Schuster, G. B.; Platz, M. S. *Adv. Photochem.* **1992**, *117*, 69.
(6) Matsumara, Y.; Shiozawa, T.; Matsushita, H.; Terao, Y. *Biol. Pharm. Bull.* **1995**, *18*, 1805.
(7) Tindall, C.; Hemminger, J. *Surf. Sci.* **1995**, *330*, 67.
(8) Bridges, A. S.; Greef, R.; Jonathan, N. B. H.; Morris, A.; Parker, G. *Surf. Rev. Lett.* **1994**, *1*, 573.
(9) Kubota, N. J. *Propul. Power* **1995**, *11*, 677.
(10) Liu, Y. L.; Hsuie, G. H.; Chiu, Y. S. *J. Appl. Polym. Sci.* **1995**, *58*, 579.
(11) Badri, M.; Mooney, H. M. *Geophysics* **1987**, *52*, 772.
(12) Bock, H.; Dammel, R. *Angew. Chem., Int. Ed. Engl.* **1987**, *26*, 504.
(13) Dammel, R. Ph.D. Thesis, University of Frankfurt, Germany 1985.
(14) Bock, H.; Dammel, R.; Aygen, S. J. *J. Am. Chem. Soc.* **1983**, *105*, 7681.
(15) Bock, H.; Dammel, R. *J. Am. Chem. Soc.* **1988**, *110*, 5261.
(16) Bock, H.; Dammel, R.; Horner, L. *Chem. Ber.* **1981**, *114*, 220.
(17) (a) Jing, W.; Zheng, S.; Xinjiang, Z.; Xiaojun, Y.; Maofa, G.; Dianxun, W.; *Angew. Chem., Int. Ed.* **2001**, *40*, 3055. (b) Dianxun, W. Private communication.
(18) See, for example: Scrivener, E. F. V., Ed. *Azides and Nitrenes*; Academic Press: New York, 1984.
(19) Geiseler, G.; Konig, W. *Z. Phys. Chem.* **1964**, *227*, 81.
(20) Dyke, J. M.; Groves, A. P.; Morris, A.; Ogden, J. S.; Dias, A. A.; Oliveira, A. M. S.; Costa, M. L.; Barros, M. T.; Cabral, M. H.; Moutinho, A. M. C. *J. Am. Chem. Soc.* **1997**, *119*, 6883.
(21) Dyke, J. M.; Groves, A. P.; Morris, A.; Ogden, J. S.; Catarino, M. I.; Dias, A. A.; Oliveira, A. M. S.; Costa, M. L.; Barros, M. T.; Cabral, M. H.; Moutinho, A. M. C. *J. Phys. Chem. A* **1999**, *103*, 8239.
(22) Hooper, N.; Beeching, L. J.; Dyke, J. M.; Morris, A.; Ogden, J. S.; Dias, A. A.; Costa, M. L.; Barros, M. T.; Cabral, M. H.; Moutinho, A. M. C. *J. Phys. Chem. A* **2002**, *106*, 9968.
(23) Bulgin, D. K.; Dyke, J. M.; Goodfellow, F.; Jonathan, N. B. H.; Lee, E. P. F.; Morris, A. *J. Electron Spectrosc. Relat. Phenom.* **1977**, *12*, 67.
(24) Turner, D. W.; Baker, C.; Baker, A. D.; Brundle, C. R. *Molecular Photoelectron Spectroscopy*; Wiley-Interscience: New York, 1971.
(25) Basch, H.; Robin, M. B.; Kuebler, N. A.; Baker, C.; Turner, D. W. *J. Chem. Phys.* **1969**, *51*, 52.
(26) Robin, M. B.; Brundle, C. R.; Kuebler, N. A.; Ellison, G. B.; Wiberg, K. B. *J. Chem. Phys.* **1972**, *57*, 1758.
(27) Scott, A. P.; Radom, L. *J. Phys. Chem.* **1996**, *100*, 16502.
(28) Pople, J. A.; Scott, A. P.; Wong, M. W.; Radom, L. *Isr. J. Chem.* **1993**, *33*, 345.
(29) Hout, R. F.; Levi, B. A.; Hehre, W. J. *J. Comput. Chem.* **1982**, *3*, 234.
(30) Pettersson, M.; Khriatchtev, L.; Jolkkonen, S.; Rasanen, M. *J. Phys. Chem. A* **1999**, *103*, 9154.
(31) Peel, J. B.; Willett, G. D. *J. Chem. Soc., Faraday Trans. II* **1975**, *71*, 1799.
(32) Eland, J. H. D. *Philos. Trans. R. Soc. London, Ser. A* **1970**, *268*, 87.
(33) Corderio, M. N. D. S.; Dias, A. A.; Costa, M. L.; Gomes, A. N. F. *J. Phys. Chem. A* **2001**, *105*, 3140.
(34) Ogden, J. S. Unpublished observations. See also, Dubost, H.; Abouaf-Marguin, L. *Chem. Phys. Lett.* **1972**, *17*, 269.
(35) Jacox, M. E.; Milligan, D. E. *J. Mol. Spectrosc.* **1975,** *56*, 333.
(36) King, C. M.; Nixon, E. R. *J. Chem. Phys.* **1968**, *48*, 1685.
(37) Cugley, J. A.; Pullen, A. D. E. *Spectrochim. Acta A* **1973**, *29*, 1665.
(38) See, for example: *NIST Chemistry WebBook*; NIST Standard Reference Database 69, March 2003 release; National Institute for Standards and Technology: Gaithersburg, MD, 2003. Also: DeFrees, D. J.; Hehre, W. J. *J. Phys. Chem.* **1978**, *82*, 391.